Long-time protection of thermal correlations in a hybrid-spin system under random telegraph noise

Fadwa Benabdallah [1], Atta Ur Rahman [2], Saeed Haddadi [3,4,*] and Mohammed Daoud [5,6]

[1] *LPHE-Modeling and Simulation, Faculty of Sciences, Mohammed V University in Rabat, Morocco*

[2] *Key Laboratory of Aerospace Information Security and Trusted Computing, Ministry of Education, School of Cyber Science and Engineering, Wuhan University, Wuhan 430072, China*

[3] *Faculty of Physics, Semnan University, P.O. Box 35195-363, Semnan, Iran*

[4] *Saeed's Quantum Information Group, P.O. Box 19395-0560, Tehran, Iran*

[5] *Department of Physics, Faculty of Sciences, Ibn Tofail University, Kénitra, Morocco*

[6] *Abdus Salam International Centre for Theoretical Physics, Strada Costiera 11, I-34151 Trieste, Italy*

(Received 18 April 2022; accepted 29 August 2022; published 15 September 2022)

The engineering features of transmitting mediums and their impact on different characteristics of a quantum system play a significant role in the efficient performance of nonlocal protocols. For this purpose, the dynamics of open quantum systems and coupling mediums remain a pathway. In this work, we investigate the dynamics of quantum correlations using negativity, uncertainty-induced nonlocality, and local quantum Fisher information in a hybrid qubit-qutrit thermal state when coupled with a magnetic field and influenced by random telegraph noise. Different features of the system parameters are taken into account while designing longer preservation of qubit-qutrit correlations. We show that the temperature has an inverse impact on the initial values of negativity, uncertainty-induced nonlocality, and local quantum Fisher information. When the magnetic field is characterized by different features, the entanglement, nonlocality, and Fisher information show a variety of dynamical maps, assuring their distinct nature. In addition, the qubit-qutrit correlations undergo repeated revivals when the configuration is restricted to the non-Markovian regime. On the other hand, an exponential drop with a single minimum is observed in the Markovian regime of the coupled field. Most importantly, our findings reveal that the present coupled fields have several advantages that can be leveraged to generate the optimal degree of entanglement, nonlocality, and local quantum Fisher information preservation in quantum dynamical maps.

DOI: 10.1103/PhysRevE.106.034122

I. INTRODUCTION

The presence of nonclassical correlations among subcomponents of a quantum state affect the efficacy of its quantum operations [1–3]. Not only the presence but the amount as well as the nature of the correlations present between the submarginal systems of a composite nonlocal system have an impact on the practical implication of nonclassical protocols. Therefore, recognition as well as the estimation of nonlocal correlations have remained a hot topic in quantum information theory [4,5]. In this regard, quantum systems, in general, can have both classical and quantum correlations. Quantum entanglement, the very well known nonclassical occurrence, has been recognized as a critical resource in several quantum information and communication procedures [6–8], including quantum computation [9], teleportation [10], cryptography [11], entanglement swapping [12], quantum private comparison protocols [13], key distribution [14], and dense coding [15], to name a few.

Nonclassical correlations of many-body systems are a rapidly expanding field with a wide range of applications, including phase transitions [16]. Many researchers have investigated quantum entanglement in thermally defined equilibrium states of spin chains exposed to magnetic fields and found interesting results [17]. The interactions of quantum systems with coupled environments usually result in loss of nonclassical correlations between the subsystems of a composite state in this regard. Realizing such decohering effects is critical in the field of quantum information and computing because it allows for efficient information transfer while avoiding the losses that come with it [18]. Decoherence effects in bipartite and tripartite qubit and qutrit systems interacting with various types of environmental strategies have been studied extensively; for example, see Refs. [19–24]. According to recent research, hybrid quantum systems, such as qubit-qutrit studies, have useful properties for preserving quantum correlations when compared to simple bipartite and tripartite states. In this case, the bipartite Heisenberg *XXX* model is one of the most promising candidates for overcoming decoherence effects caused by the environment, as it has demonstrated a high-tolerance capacity for preserving quantum correlations over longer periods [25]. The features of the quantum mixed spin system are also appealing, in addition to the conventional spin-1/2 system. In this regard, a quasi-single-dimensional chain, $A\mathrm{Cu(pbaOH)(H_2O)_3 \cdot 2H_2O}$, with every subunit carrying two different spins $(S, 1/2)$, has been produced for an inorganic compound [26]. The *A*Cu compounds have antiferromagnetic interactions and can be thought of as a Heisenberg mixed spin $(S, 1/2)$ with antiferromagnetic

*Corresponding author: saeed@ssqig.com

interactions. A mixed spin $(1, 1/2)$ model may be used to represent the bimetallic chain of the NiCu compound [26]. In the present case, we aim to investigate quantum correlations encoded in the thermal qubit-qutrit mixed *XXZ* spin chain model under the influence of an external magnetic field, the Dzyaloshinskii-Moriya (DM) interaction, and exchange coupling constant.

The study of spin chains that are coupled to external magnetic fields, with a focus on magnetic and other related effects, has sparked a lot of interest in recent years [27–32]. This appears to be ideal because the environment in which quantum systems are coupled is typically made up of various types of instabilities. Random telegraph (RT) noise could be caused by charge trapping at the surfaces of thin films; for instance, see Ref. [33]. Thermal fluctuations in various solid-state and superconducting substances cause low-frequency noise, also known as power-law noise [34]. Another instability is fractional Gaussian and Ornstein-Uhlenbeck noises, which are caused by the random motion of particles in a medium [34]. In this case, we will focus on the dephasing effects caused by the RT noise because it is prevalent in many quantum information processing protocols [35,36]. It has also been extensively researched theoretically to characterize system-environment interactions [37–39]. Chemical processes such as molecule fluorescence [39], nonlocal correlation degradation in the presence of low-frequency noise [40], and frequency amplifications [41] have all been investigated using noise. In addition, the experimental study of RT noise revealed dephasing effects in the dynamics of open quantum systems, resulting in rapid nonlocal correlation degradation [42]. In this case, we consider a hybrid environment in which the dynamics of quantum correlations in a Heisenberg *XXZ* spin chain are influenced by both the unstable effects of external magnetic fields and the RT noise. This will not only set us apart from previous research, but it will also lead to more precise results for real-world quantum protocols, such as dephasing effects.

Quantum correlation measures such as entanglement witnesses [43], concurrence [44], and quantum discord have all been developed in recent decades [45]. Quantum correlations between subparticles can be found using any of these metrics [46]. Updated versions or entirely new quantum correlation metrics have recently been derived, which can detect quantum correlations beyond quantum entanglement. Geometric quantum discord [47], local quantum uncertainty [48], local quantum Fisher information (LQFI) [49], and measurement-induced nonlocality [50] are examples of quantum correlation criteria. Recent quantifiers have revealed nonlocal correlations that were heretofore undetectable by previous measures. As a result, quantum operations became more efficient and precise. Thus, in the current study, we aim to include quantum correlation quantifiers such as negativity [51], uncertainty-induced nonlocality (UIN) [52], and LQFI [49], which are more reliable and are easily computable measures. The use of negativity is motivated by the fact that it is one of the most successful entanglement monotones [53,54]. The UIN will help determine the amount of nonlocality in the thermal state [52]. In addition to providing insight into quantum correlation preservation, LQFI can be used to characterize different parameters and their role in quantum correlation preservation [55].

This paper investigates the dynamics of quantum correlations in a hybrid thermal qubit-qutrit system exposed to an external magnetic field influenced by RT noise, temperature, and DM interaction [56]. Quantum systems are generally very sensitive to thermal fluctuations; therefore, the related quantum correlations will be degraded quickly if temperature effects are not controlled precisely. Previous research [57] has mainly focused on the external magnetic field effect and DM interaction strength. However, in the current study, besides DM interaction, we include the effects of exchange coupling, and manipulation of the associated Markovianity and non-Markovianity of the fields to induce longer qubit-qutrit correlations. To estimate the quantum correlations, we plan to use negativity, UIN, and LQFI, and a comparison of each measure to evaluate quantum correlations will also be drawn.

The paper is organized as follows: We describe the physical model in detail in Sec. II. Section III introduces the quantum correlation estimators, and Sec. IV presents the main results and related discussion. We express some final remarks in Sec. V and the conclusion is given in Sec. VI.

II. PHYSICAL MODEL: THE EXACTLY SOLVABLE CASE

In this section, let us consider a qubit-qutrit mixed spin $(1/2, 1)$ Heisenberg *XXZ* chain model under the presence of an inhomogeneous magnetic field, DM interaction, and exchange coupling constant. The self-Hamiltonian describing the mentioned system reads [58]

$$H = H_{XXZ} = J\left[\left(s_1^x S_2^x + s_1^y S_2^y + \Delta s_1^z S_2^z\right) + D_z\left(s_1^x S_2^y - s_1^y S_2^x\right)\right] + \mu_B B\left(s_1^z + S_2^z\right) - b\left(s_1^z - S_2^z\right), \tag{1}$$

where s_1^α and S_2^α $(\alpha = x, y, z)$ denote spatial components of the spin-1/2 (qubit) and spin-1 (qutrit) operators, respectively. The coupling constant J denotes the Heisenberg exchange interaction between spin-1/2 and spin-1 particles. Positive range $J > 0$ corresponds to the antiferromagnetic interaction between sites of the model while $J < 0$ indicates the ferromagnetic case. Besides, the parameter Δ represents the *XXZ* exchange anisotropy in this exchange interaction, and the parameter D_z refers to the strength of DM interaction oriented along the z direction. The parameter B denotes a static external magnetic field and μ_B is the Bohr magneton [53,54]. Finally, b indicates the degree of inhomogeneity of the magnetic field. By straightforward calculations, the eigenvalues of the bipartite model with self-Hamiltonian (1) are obtained as follows (setting $\hbar = 1$) [58]:

$$\begin{aligned} E_{1,2} &= \tfrac{1}{2}(\mp b \mp 3\mu_B B + J\Delta), \\ E_{3,4} &= \tfrac{1}{4}(2b + 2\mu_B B - J\Delta \mp \omega^-), \\ E_{5,6} &= \tfrac{1}{4}(-2b - 2\mu_B B - J\Delta \mp \omega^+), \end{aligned} \tag{2}$$

with $\omega^\pm = \sqrt{(4b)^2 + 2(2J)^2 + 2(2D_z J)^2 \pm 8bJ\Delta + (J\Delta)^2}$. The corresponding orthogonal eigenstates are respectively given as follows:

$$|\psi_1\rangle = |\uparrow, \Uparrow\rangle,\ |\psi_2\rangle = |\downarrow \Downarrow\rangle,$$

$$|\psi_3\rangle = \frac{1}{\sqrt{1 + |\eta_+|^2}}(\eta_+|\downarrow \bigcirc\rangle + |\uparrow\Downarrow\rangle),$$

$$|\psi_4\rangle = \frac{1}{\sqrt{1+|\eta_-|^2}}(\eta_-|\downarrow\bigcirc\rangle + |\uparrow\Downarrow\rangle),$$
$$|\psi_5\rangle = \frac{1}{\sqrt{1+|\vartheta_+|^2}}(\vartheta_+|\downarrow\Uparrow\rangle + |\uparrow\bigcirc\rangle),$$
$$|\psi_6\rangle = \frac{1}{\sqrt{1+|\vartheta_-|^2}}(\vartheta_-|\downarrow\Uparrow\rangle + |\uparrow\bigcirc\rangle), \tag{3}$$

where $\eta_\pm = \frac{-4b+J\Delta\mp\omega^-}{2\sqrt{2}J(D_z+i)}i$ and $\vartheta_\pm = -\frac{4b+J\Delta\pm\omega^+}{2\sqrt{2}J(D_z+i)}i$. Moreover, $|\uparrow\rangle$ and $|\downarrow\rangle$ represent the eigenbasis of the z component of spin-1/2 operator s^z whereas $|\Uparrow\rangle$, $|\bigcirc\rangle$, and $|\Downarrow\rangle$ are known to be the eigenbasis of spin-1 operators S^z along the z component.

At the equilibrium (canonical ensemble), the initial quantum state of the mixed spin-(1/2, 1) Heisenberg chain (1) can be represented by the density operator, namely $\rho(0, T) = \exp(-\beta H)/Z$, which is expressed in terms of the partition function $Z = \mathrm{Tr}[\exp(-\beta H)]$, where $\beta = 1/k_B T$ is the inverse of the thermodynamic temperature T, and k_B is the Boltzmann constant. For the sake of simplicity, the parameter J is set to be the unit of energy. To investigate the time evolution of temperature-dependent nonclassical correlations, let us consider the well-known local non-Markovian dephasing behavior introduced by Daffer *et al.* [59]. This model has recently been widely used to study the sudden change in the dynamics of quantum correlations [60]. Now, we can consider a colored noise dephasing model with dynamics described by the following master equation at scaled time t [59–61],

$$\dot{\rho}(t) = \mathcal{K}\mathcal{L}\rho(t), \tag{4}$$

where $\mathcal{K}$ is a time-dependent integral operator, satisfying the relation

$$\mathcal{K}\phi = \int_0^t k(t-t')\phi(t')dt', \tag{5}$$

where $k(t-t')$ is the kernel function which regulates the nature of the environment, $\mathcal{L}$ is the Lindblad superoperator that describes the dynamics induced via the interaction with the environment, and $\rho(t)$ is the density operator of the principal system. It is important to note that without applying the time-dependent integral operator $\mathcal{K}$, the master equation (4) with Markovian approximation becomes dominant. Also, the mentioned master equation can be employed if we consider a bipartite qubit-qutrit system interacting with a reservoir having the properties of RT noise. To this end, we can consider the stochastic Hamiltonian as [59–62]

$$\delta H(t) = \delta\omega_A(t)s_A^z + \delta\omega_B(t)S_B^z, \tag{6}$$

where ω_n with $n = \{A, B\}$ are the independent random variables obeying the statistic of a RT signal defined as $\omega_n(t) = a_n(-1)^{m_n(t)}$, where $m_n(t)$ has a Poisson distribution with a mean equal to $t/2\tau_n$, and a_n is known as the switching amplitude taking the values $\pm a_n$. Here, we assume $a_A = a_B = a$ and $\tau_A = \tau_B = \tau$. Using the time-dependent stochastic Hamiltonian (6), the represented correlation function of the RT signal using the stochastic variables reads

$$\langle\omega_n(t)\omega_{n'}(t')\rangle = \delta_{n,n'}a^2\exp(-\gamma|t-t'|), \tag{7}$$

where $\langle\cdots\rangle$ stands for the ensemble average whereas $\gamma = 1/\tau$ is known as the switching rate, which characterizes the spectral width of the coupling with the environment [63]. The time evolution of the density matrix describing the qubit-qutrit system (6) is given by taking ensemble averages over the stochastic noise variables as follows,

$$\rho(t, T) = \langle U(t)\rho(0, T)U^\dagger(t)\rangle, \tag{8}$$

with $\rho(0, T) = \exp(-\beta H)/Z$ and in terms of the unitary operator $U(t)$ obtained from the stochastic Schrödinger equation as

$$U(t) = \mathcal{T}\exp\left[-i\int_0^t H(t')dt'\right], \tag{9}$$

where $\mathcal{T}$ is the time-ordering operator. In general, within the framework of the classical treatment, the environmental effects on a quantum system give rise to the stochastic fluctuations in the Hamiltonian of the quantum system as

$$H(t) = H + \delta H(t). \tag{10}$$

Note that the unitary operator contains both the contributions from the self-Hamiltonian and the stochastic Hamiltonian.

Many approaches have been devoted to studying the dynamical behaviors of a given quantum system such as the master equation [64,65] and decomposition by Kraus operators [66]. In the current case, we find that it is more suitable to use the Kraus operators to probe the quantum dynamics of the model under consideration [66]. The Kraus operators describing the RT noise dynamical map and related effects on the qubit-qutrit system are respectively provided by [60,62]

$$K_1^A = \sqrt{\frac{1+\Lambda(\nu)}{2}}I_A, \quad K_2^A = \sqrt{\frac{1-\Lambda(\nu)}{2}}s_A^z, \tag{11}$$

and

$$K_1^B = \sqrt{\frac{1+\Lambda(\nu)}{2}}I_B, \quad K_2^B = \sqrt{\frac{1-\Lambda(\nu)}{2}}S_B^z,$$
$$K_3^B = \sqrt{\frac{1+\Lambda(\nu)}{2}}\mathcal{S}_B, \tag{12}$$

where K_i satisfies the completeness condition guaranteeing that the evolution is trace-preserving and represents the influence of statistical noise which can be global or local in scope, and where the index runs over the number of elements required for the decomposition. Besides, these operators satisfy the normalization condition $\sum_i K_i^\dagger K_i = I$ with

$$\mathcal{S}_B = \tfrac{1}{2}\left(S_B^x S_B^x + S_B^y S_B^y - S_B^z S_B^z\right), \tag{13}$$

and I_A (I_B) is the identity operator acting on the qubit (qutrit) subspace. The term $\Lambda(\nu)$ is generally called the dephasing function and has the form [59–61]

$$\Lambda(\nu) = \frac{1}{\mu}\exp(-\nu)[\sin(\mu\nu) + \mu\cos(\mu\nu)], \tag{14}$$

in which $\mu = \sqrt{(4a\tau)^2 - 1}$ and $\nu = t/2\tau$ is the scaled time. With no tunneling coupling in the Hamiltonian, the quantum dynamics of a qubit-qutrit system are described by the dephasing function in the form of Eq. (14), which displays the non-Markovian behavior in the strong-coupling regime ($\tau > 2a$) and shows Markovian behavior in the weak-coupling

regime ($\tau < 2a$). Herein, the qubit-qutrit system is equally coupled to all environment frequencies. In the case of RT noise, our system prefers specific frequencies. Accordingly, a is the coupling strength of the qubit-qutrit system with the environment whereas τ determines which frequencies the mentioned system prefers most. Enhancing both a and $\gamma = 1/\tau$ corresponds to a more noisy environment. Hence, the dimensionless quantity $a\tau$ is the significant term that determines the number of fluctuations [59]. From now on, let us consider $a = 1$ for simplicity. As a result, the parameter τ will exclusively be the dominant factor to determine the amount of information exchange between the qubit-qutrit system and the environment.

Now, we derive the density matrix of the system having obvious entanglement as well as the quantum correlation sudden death and birth phenomenon. In order to exhibit entanglement sudden death (ESD) and entanglement sudden birth (ESB) in the qubit-qutrit class state, we consider dephasing RT noise alone acting on subsystems that are dynamically isolated from each other.

The most general time-evolved open-system density matrix expressible in the operator-sum decomposition has the form [60–62]

$$\rho(t,T) = \sum_{i=1}^{2}\sum_{j=1}^{3}\left(K_i^A \otimes K_j^B\right)\rho(0,T)\left(K_i^A \otimes K_j^B\right)^{\dagger}. \quad (15)$$

Note that only when the stochastic Hamiltonian $\delta H(t)$ is commutative with the self-Hamiltonian H and the stochastic Hamiltonian is in the energy eigenvalues of the system, the quantum system undergoes dephasing and the density matrix can be expressed in terms of the dephasing function $\Lambda(\nu)$. Otherwise, the density matrix of the system cannot be generally expressed in the Kraus operator representation in terms of the dephasing function. After straightforward calculation, the time and temperature dependencies of our qubit-qutrit density matrix can be written in the computational basis $\{|\downarrow,\Downarrow\rangle\}$, $\{|\downarrow,\bigcirc\rangle\}$, $\{|\downarrow,\Uparrow\rangle\}$, $\{|\uparrow,\Downarrow\rangle\}$, $\{|\uparrow,\bigcirc\rangle\}$, $\{|\uparrow,\Uparrow\rangle\}$ as follows,

$$\rho(t,T) = \frac{1}{Z}\begin{bmatrix} \rho_{1,1} & 0 & 0 & 0 & 0 & 0 \\ 0 & \rho_{2,2} & 0 & \rho_{2,4} & 0 & 0 \\ 0 & 0 & \rho_{3,3} & 0 & \rho_{3,5} & 0 \\ 0 & \rho_{2,4}^{*} & 0 & \rho_{4,4} & 0 & 0 \\ 0 & 0 & \rho_{3,5}^{*} & 0 & \rho_{5,5} & 0 \\ 0 & 0 & 0 & 0 & 0 & \rho_{6,6} \end{bmatrix}, \quad (16)$$

where

$$\rho_{1,1} = \exp(-\beta E_2),\ \rho_{6,6} = \exp(-\beta E_1),$$

$$\rho_{2,2} = \frac{|\eta_+|^2}{1+|\eta_+|^2}\exp(-\beta E_3) + \frac{|\eta_-|^2}{1+|\eta_-|^2}\exp(-\beta E_4),$$

$$\rho_{2,4} = \frac{1}{2}[1+\Lambda(\nu)] \times\left[\frac{\eta_+}{1+|\eta_+|^2}\exp(-\beta E_3) + \frac{\eta_-}{1+|\eta_-|^2}\exp(-\beta E_4)\right],$$

$$\rho_{3,3} = \frac{|\vartheta_+|^2}{1+|\vartheta_+|^2}\exp(-\beta E_5) + \frac{|\vartheta_-|^2}{1+|\vartheta_-|^2}\exp(-\beta E_6),$$

$$\rho_{3,5} = \frac{1}{2}[1+\Lambda(\nu)] \times\left[\frac{\vartheta_+}{1+|\vartheta_+|^2}\exp(-\beta E_5) + \frac{\vartheta_-}{1+|\vartheta_-|^2}\exp(-\beta E_6)\right],$$

$$\rho_{4,4} = \frac{1}{1+|\eta_+|^2}\exp(-\beta E_3) + \frac{1}{1+|\eta_-|^2}\exp(-\beta E_4),$$

$$\rho_{5,5} = \frac{1}{1+|\vartheta_+|^2}\exp(-\beta E_5) + \frac{1}{1+|\vartheta_-|^2}\exp(-\beta E_6), \quad (17)$$

and the partition function Z is given by

$$Z = \sum_{j=1}^{6}\exp(-\beta E_j). \quad (18)$$

Notably, the density matrix of the composite qubit-qutrit system has been expressed as $\rho(t,T)$ given in Eq. (16), implying that the operators s_A^z and S_B^z in the stochastic Hamiltonian are in the energy eigenbasis of the self-Hamiltonian of the qubit and the qutrit subsystems, respectively.

III. QUANTUM CORRELATION INDICATORS

A. Negativity

To investigate the amount of quantum entanglement of a system with spin $S > 1/2$, one may employ a quantity known as negativity $N(\rho)$ [67]. This quantifier has been proven to be one of the most suitable quantifiers, which can be easily computable for any arbitrary pure or mixed state. It is based on the concept of the Peres and Horodecki separability criterion [68,69], in which a negative partial transpose is a necessary condition for the system entanglement. The negativity $N(\rho)$ is defined through the absolute sum of all negative eigenvalues ϑ_i of the partial-transposed density matrix ρ^{T_A} concerning the spin-1/2 subsystem (A denotes the first subsystem). Generally, it reads [67]

$$N(\rho) = \sum_i |\vartheta_i|. \quad (19)$$

The negativity can also be identified via the Schatten 1-norm (trace norm) as below [67],

$$N(\rho) = \frac{||\rho^{T_A}||_1 - 1}{2}, \quad (20)$$

where the term $||X||_1 = \mathrm{Tr}(\sqrt{X^{\dagger}X})$ presents the trace norm for any Hermitian operator X. It is worth mentioning that for maximally entangled states, the negativity is equal to half $[N(\rho) = 1/2]$, whereas $N(\rho) = 0$ corresponds to completely separable (factorizable) states. However, let us consider here a rescaled form of the negativity definition as $\mathcal{N}(\rho) = 2 \times N(\rho)$ for our calculations. Therefore, we will have $0 \leqslant \mathcal{N}(\rho) \leqslant 1$.

In order to evaluate the time and temperature dependencies of the negativity of a qubit-qutrit system $\rho(t,T)$ given in Eq. (16), one needs first to obtain the negative eigenvalues of the partial-transposed density matrix of the total system. To do this, a partial transposition with respect to states of the spin-1/2 gives the partially transposed density matrix $[\rho(t,T)]^{T_A}$. In the computational basis, the thermal-time evolved partial

transposed density matrix $[\rho(t,T)]^{T_A}$ takes the form

$$[\rho(t,T)]^{T_A}=\frac{1}{Z}\begin{pmatrix}\rho_{1,1}&0&0&0&\rho_{2,4}&0\\0&\rho_{2,2}&0&0&0&\rho_{3,5}\\0&0&\rho_{3,3}&0&0&0\\0&0&0&\rho_{4,4}&0&0\\\rho^*_{2,4}&0&0&0&\rho_{5,5}&0\\0&\rho^*_{3,5}&0&0&0&\rho_{6,6}\end{pmatrix}. \tag{21}$$

Now, the possible negative eigenvalues of the state $[\rho(t,T)]^{T_A}$ (21) are gained as

$$\vartheta_1(t,T)=\frac{1}{2Z}[(\rho_{1,1}+\rho_{5,5})-\sqrt{(\rho_{1,1}-\rho_{5,5})^2+4|\rho_{2,4}|^2}], \tag{22}$$

$$\vartheta_2(t,T)=\frac{1}{2Z}[(\rho_{2,2}+\rho_{6,6})-\sqrt{(\rho_{2,2}-\rho_{6,6})^2+4|\rho_{3,5}|^2}], \tag{23}$$

and therefore, the negativity of our state can be expressed as

$$\mathcal{N}(\rho(t,T))=2[\max\{0,-\vartheta_1(t,T)\}+\max\{0,-\vartheta_2(t,T)\}]. \tag{24}$$

B. Uncertainty-induced quantum nonlocality

The UIN is a promising discord-like quantifier linked to the Wigner-Yanase skew information (WYSI) concept [70]. This nonclassical correlation quantifier is defined as the maximal skew information achievable between a given bipartite quantum state ρ and local commuting observable $K^C=K^C_{\rm A}\otimes I_{\rm B}$. The UIN with respect to subsystem A can be expressed in terms of WYSI for a given state ρ as [71,72]

$$\mathcal{U}_C(\rho)=\max_{K^C_{\rm A}\otimes I_{\rm B}}\mathcal{I}\big(\rho,K^C_{\rm A}\otimes I_{\rm B}\big), \tag{25}$$

where the maximum is taken over the set of all observables, $K^C=K^C_{\rm A}\otimes I_{\rm B}$, that commutes with the reduced density matrix ρ^A, where $K^C_{\rm A}$ is a Hermitian operator acting on subsystem A with a nondegenerate spectrum Λ. Moreover, $I_{\rm B}$ is the identity operator acting on subsystem B, while $\mathcal{I}$ is the skew information associated with the density matrix and defined as

$$\mathcal{I}(\rho,K^\Lambda)=-\tfrac{1}{2}{\rm Tr}([\sqrt{\rho},K^\Lambda]^2), \tag{26}$$

which is a measure of the noncommutativity between the state ρ and the observable K^Λ. Note that $\mathcal{I}$ is non-negative and nonincreasing under classical mixing [73]. For a $2\otimes d$ (qubit-qudit) bipartite quantum system, the compact formula of UIN turns out to be

$$\mathcal{U}_C(\rho)=\begin{cases}1-\omega_{\min}(\mathcal{W}_{\rm AB}),\vec{r}=\vec{0},\\1-\frac{1}{\|\vec{r}\|^2}\vec{r}\mathcal{W}_{\rm AB}\vec{r}^{\,T},\vec{r}\neq\vec{0},\end{cases} \tag{27}$$

where $\vec{r}=[r_i]$ is the Bloch vector of the density matrix ρ, whose elements are calculated by $r_i={\rm Tr}(\rho[\sigma_i\otimes I])$. The superscript T stands for the transpose operation and $\omega_{\min}(\mathcal{W}_{\rm AB})$ stands for the least eigenvalue of the 3×3 symmetric matrix $\mathcal{W}_{\rm AB}$ whose elements are given by

$$(\mathcal{W}_{\rm AB})_{\alpha\beta}={\rm Tr}\big[\sqrt{\rho}\big(\sigma^\alpha_{\rm A}\otimes I_{\rm B}\big)\sqrt{\rho}\big(\sigma^\beta_{\rm A}\otimes I_{\rm B}\big)\big], \tag{28}$$

where $\sigma^{\alpha(\beta)}_{\rm A}$ with $\alpha(\beta)=\{x,y,z\}$ represent the Pauli operators of the subsystem A. The UIN is a reliable quantifier of quantum correlations and it has been demonstrated that this measure satisfies the full physical requirements of a measure of quantum correlations [71,72]. It is clear that having the matrix $\mathcal{W}_{\rm AB}$, one can easily evaluate the UIN for qubit-qutrit quantum systems contrarily to the quantum discord based on von Neumann entropy [73]. This is quite an easy task compared with the complicated minimization process over parameters due to the local measurements [48,65]. However, for the pure bipartite states, the UIN reduces to the linear entropy of the reduced densities of the subsystems and vanishes for classically correlated state [48]. Moreover, it is invariant under local unitary operations and nonincreasing under the local operation on the unmeasured subsystem B [48]. To determine the analytical expression of the UIN (27), it is necessary to compute the eigenvalues of the matrix $\mathcal{W}_{\rm AB}$ (28). For that, one needs to determine both the eigenvalues and the corresponding eigenvectors associated with the density matrix $\rho(t,T)$ in Eq. (16), viz.,

$$\begin{aligned}&\lambda_{1,6}=\tfrac{1}{2}\big(\xi_1\pm\sqrt{\xi_1^2-4d_1}\big),\\&\lambda_{2,3}=\tfrac{1}{2}\big(\xi_2\mp\sqrt{\xi_2^2-4d_2}\big),\quad\lambda_{4,5}=\tfrac{1}{2}\big(\xi_3\mp\sqrt{\xi_3^2-4d_3}\big),\end{aligned} \tag{29}$$

where

$$\begin{aligned}&\xi_1=\rho_{11}+\rho_{66},\quad\xi_2=\rho_{22}+\rho_{44},\quad\xi_3=\rho_{33}+\rho_{55},\\&d_1=\rho_{11}\rho_{66},\quad d_2=\rho_{22}\rho_{44}-|\rho_{24}|^2,\\&d_3=\rho_{33}\rho_{55}-|\rho_{35}|^2,\end{aligned} \tag{30}$$

and the associated eigenvectors are

$$\begin{aligned}&|\lambda_1\rangle=|\uparrow\Uparrow\rangle,\quad|\lambda_6\rangle=|\downarrow\Downarrow\rangle,\\&|\lambda_{2,3}\rangle=\frac{1}{\sqrt{1+|\upsilon_\pm|^2}}(\upsilon_\pm|\uparrow\bigcirc\rangle+|\downarrow\Uparrow\rangle),\\&|\lambda_{4,5}\rangle=\frac{1}{\sqrt{1+|\eta_\pm|^2}}(\eta_\pm|\uparrow\Downarrow\rangle+|\downarrow\bigcirc\rangle),\end{aligned} \tag{31}$$

where

$$\upsilon_\pm=\frac{1}{2\rho^*_{2,4}}[\rho_{2,2}-\rho_{4,4}\pm\sqrt{(\rho_{2,2}-\rho_{4,4})^2+4|\rho_{2,4}|^2}], \tag{32}$$

$$\eta_\pm=\frac{1}{2\rho^*_{3,5}}[\rho_{3,3}-\rho_{5,5}\pm\sqrt{(\rho_{3,3}-\rho_{5,5})^2+4|\rho_{3,5}|^2}]. \tag{33}$$

The square root of the density matrix can be written in the computational basis as follows,

$$\sqrt{\rho(t,T)}=\begin{pmatrix}\alpha_{11}&0&0&0&0&0\\0&\alpha_{22}&0&\alpha_{24}&0&0\\0&0&\alpha_{33}&0&\alpha_{35}&0\\0&\alpha^*_{24}&0&\alpha_{44}&0&0\\0&0&\alpha^*_{35}&0&\alpha_{55}&0\\0&0&0&0&0&\alpha_{66}\end{pmatrix}, \tag{34}$$

where

$$\alpha_{11} = \frac{1}{2}(\sqrt{\xi_1 + 2\sqrt{d_1}} + \sqrt{\xi_1 - 2\sqrt{d_1}}),$$
$$\alpha_{66} = \frac{1}{2}(\sqrt{\xi_1 + 2\sqrt{d_1}} - \sqrt{\xi_1 - 2\sqrt{d_1}}),$$
$$\alpha_{22} = \frac{\rho_{22} + \sqrt{d_2}}{\sqrt{\xi_2 + 2\sqrt{d_2}}}, \quad \alpha_{24} = \frac{\rho_{24}}{\sqrt{\xi_2 + 2\sqrt{d_2}}},$$
$$\alpha_{33} = \frac{\rho_{33} + \sqrt{d_3}}{\sqrt{\xi_3 + 2\sqrt{d_3}}}, \quad \alpha_{35} = \frac{\rho_{35}}{\sqrt{\xi_3 + 2\sqrt{d_3}}},$$
$$\alpha_{44} = \frac{\rho_{44} + \sqrt{d_2}}{\sqrt{\xi_2 + 2\sqrt{d_2}}}, \quad \alpha_{55} = \frac{\rho_{55} + \sqrt{d_3}}{\sqrt{\xi_3 + 2\sqrt{d_3}}}. \tag{35}$$

After some straightforward calculations, the eigenvalues of the matrix $\mathcal{W}_{\mathrm{AB}}$ (28) are given as

$$\mathcal{W}_{11} = \mathcal{W}_{22} = 2(\alpha_{11}\alpha_{44} + \alpha_{22}\alpha_{55} + \alpha_{33}\alpha_{66}), \tag{36}$$

$$\mathcal{W}_{33} = \sum_{i=1}^{6} \alpha_{ii}^2 - 2(|\alpha_{24}|^2 + |\alpha_{35}|^2). \tag{37}$$

By using Eq. (27), the UIN for the density matrix $\rho(t, T)$ in Eq. (16) turns out to be (since $\vec{r} \neq \vec{0}$)

$$\mathcal{U}(\rho(t, T)) = 1 - \frac{1}{|r_3|^2} r_3 \mathcal{W}_{33} r_3^*, \tag{38}$$

with $r_3 = \rho_{1,1} + \rho_{2,2} + \rho_{3,3} - \rho_{4,4} - \rho_{5,5} - \rho_{6,6}$.

C. Local quantum Fisher information

Assume a qubit-qutrit quantum state, namely ρ_κ, which depends basically on an arbitrary parameter κ. Now, in order to illustrate the information about κ from ρ_κ, it is enough to perform a set of generalized quantum measurements, that is, positive-operator-valued measures $M = \{M_\theta | M_\theta \geqslant 0\}$, satisfying $\sum_\theta M_\theta = I_d$. Mathematically, the QFI is defined as [74,75]

$$\mathcal{F}(\rho_\kappa) = \tfrac{1}{4}\mathrm{Tr}\left[\rho_\kappa \mathcal{L}_\kappa^2\right], \tag{39}$$

where $\mathcal{L}_\kappa$ denotes the symmetric logarithmic derivative operator such that

$$\frac{\partial \rho_\kappa}{\partial \kappa} = \frac{1}{2}(\mathcal{L}_\kappa \rho_\kappa + \rho_\kappa \mathcal{L}_\kappa). \tag{40}$$

Let us assume that the initial density operator $\rho_\kappa(0)$ can be evolved through a unitary evolution, namely $\mathcal{U}_\kappa = e^{-iH\kappa}$ as $\rho_\kappa = \mathcal{U}_\kappa \rho_\kappa(0) \mathcal{U}_\kappa^\dagger$. Therefore, the QFI employing the Hermitian operator H is defined as [76]

$$\mathcal{F}(\rho_\kappa, H) = \frac{1}{2} \sum_{\alpha \neq \beta} \frac{(\lambda_\alpha - \lambda_\beta)^2}{\lambda_\alpha + \lambda_\beta} |\langle \lambda_\alpha | H | \lambda_\beta \rangle|^2, \tag{41}$$

where $\rho_\kappa = \sum_i \lambda_i |\lambda_i\rangle\langle\lambda_i|$. Recently, another concept, i.e., the LQFI, has been examined based on QFI and it has attracted a great deal of attention since it defines a quantifier of nonclassical correlation using some local measurements applied on one part of the quantum state. Indeed, assume that the dynamics already mentioned is ruled now by a local transformation, that is, $e^{-i\kappa H_A}$, of a local Hamiltonian $H_A = H_a \otimes I_B$. Therefore, the LQFI is defined as [77]

$$\mathcal{F}(\rho_\kappa, H_A) = \mathrm{Tr}\left[\rho H_A^2\right] - \sum_{\alpha \neq \beta} \frac{2\lambda_\alpha \lambda_\beta}{\lambda_\alpha + \lambda_\beta} |\langle \lambda_\alpha | H_A | \lambda_\beta \rangle|^2. \tag{42}$$

As we have already pointed out the central idea behind using the LQFI is to consider it a good quantifier of nonclassical correlations. The LQFI is defined as the minimum of QFI overall local Hamiltonian H_A acting on the part A as

$$\mathcal{Q} = \min_{H_A} \mathcal{F}(\rho_\kappa, H_A). \tag{43}$$

Obviously, if one rewrites the local Hamiltonian in terms of Pauli matrices, that is, $\vec{\sigma} = (\sigma_1, \sigma_2, \sigma_3)$, and choosing the local observable $H_a = \vec{\sigma} \cdot \overrightarrow{r}$ with $|\overrightarrow{r}| = 1$, then the first term on the right-hand side of Eq. (42) is exactly corresponding to the unity, while the second term turns out to be [77–80]

$$\sum_{\alpha \neq \beta} \frac{2\lambda_\alpha \lambda_\beta}{\lambda_\alpha + \lambda_\beta} |\langle \lambda_\alpha | H_A | \lambda_\beta \rangle|^2$$
$$= \sum_{\alpha \neq \beta} \sum_{k=l=1}^{3} \frac{2\lambda_\alpha \lambda_\beta}{\lambda_\alpha + \lambda_\beta} \langle \lambda_\alpha | \sigma_k \otimes I_B | \lambda_\beta \rangle \langle \lambda_\beta | \sigma_l \otimes I_B | \lambda_\alpha \rangle$$
$$= \overrightarrow{r}^\dagger \cdot P \cdot \overrightarrow{r}, \tag{44}$$

where the elements of the symmetric matrix P are given by

$$P_{k,l} = \sum_{\alpha \neq \beta} \frac{2\lambda_\alpha \lambda_\beta}{\lambda_\alpha + \lambda_\beta} \langle \lambda_\alpha | \sigma_k \otimes I_B | \lambda_\beta \rangle \langle \lambda_\beta | \sigma_l \otimes I_B | \lambda_\alpha \rangle. \tag{45}$$

Hence, the minimum over all unit of vectors $\vec{r}$ coincides with the maximum eigenvalues of P, $\lambda_{\max}^P$. Finally, the LQFI for qubit-qutrit systems is obtained in the following form [49,78–80],

$$\mathcal{Q}(\rho) = 1 - \lambda_{\max}^P. \tag{46}$$

Notice that the above formula is non-negative, invariant under any local unitary operation, and vanishes for classically correlated states. In addition, in the case of pure quantum states, the LQFI coincides with the geometric discord [49]. After some straightforward calculations and using the eigenvalues and eigenvectors calculated in Eqs. (29) and (31), the analytical expression of LQFI for our qubit-qutrit state (16) is obtained as

$$\mathcal{Q}(\rho(t, T)) = 1 - \max\{P_{11}, P_{22}, P_{33}\}, \tag{47}$$

where $P_{ii} (i = 1, 2, 3)$ are calculated analytically from Eq. (45). They are given by

$$P_{11} = P_{22} = 4\Bigg[\frac{\lambda_1 \lambda_2}{(\lambda_1 + \lambda_2)(1 + |\upsilon_+|^2)} + \frac{\lambda_1 \lambda_3}{(\lambda_1 + \lambda_3)(1 + |\upsilon_-|^2)}$$
$$+ \frac{\lambda_4 \lambda_6 |\eta_+|^2}{(\lambda_4 + \lambda_6)(1 + |\eta_+|^2)} + \frac{\lambda_5 \lambda_6 |\eta_-|^2}{(\lambda_5 + \lambda_6)(1 + |\eta_-|^2)}$$

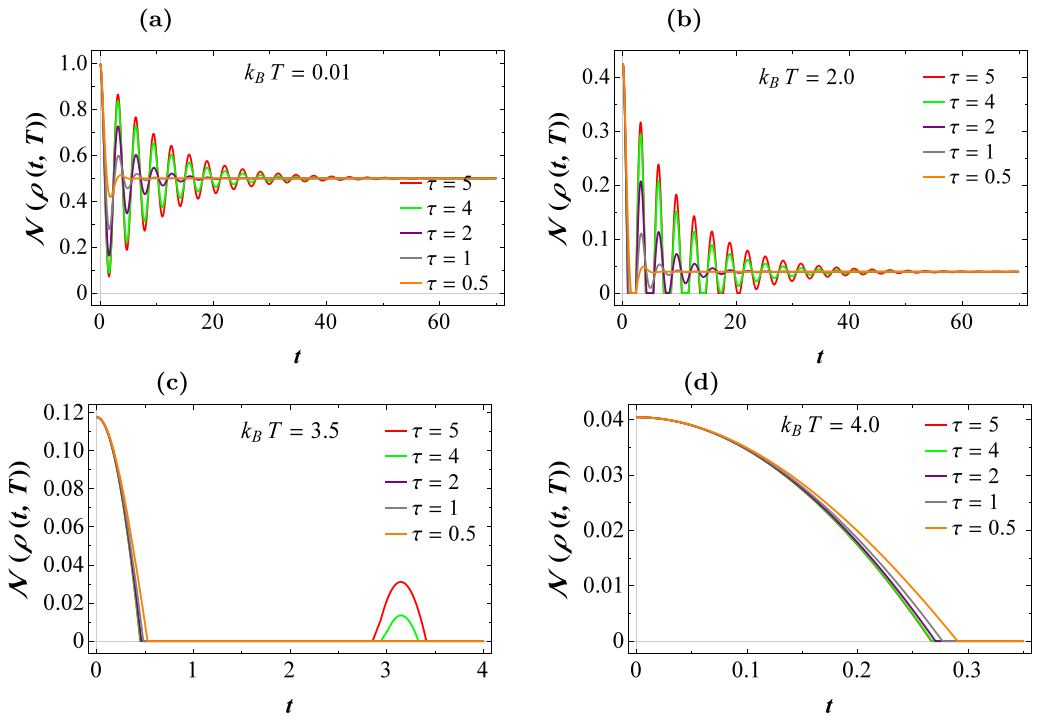

FIG. 1. Dynamics of the negativity versus time parameter t for $a = 1$ by considering a few different values of τ at different values of the temperature $k_B T/J$, assuming fixed $\mu_B B/J = 0.5$, $D_z/J = 6$, $\Delta/J = 0.5$ when $b/J = 0$.

$$+\frac{\lambda_2|\upsilon_+|^2}{(1+|\upsilon_+|^2)}\left(\frac{\lambda_4}{(\lambda_2+\lambda_4)(1+|\eta_+|^2)}+\frac{\lambda_5}{(\lambda_2+\lambda_5)(1+|\eta_-|^2)}\right)$$
$$+\frac{\lambda_3|\upsilon_-|^2}{(1+|\upsilon_-|^2)}\left(\frac{\lambda_4}{(\lambda_3+\lambda_4)(1+|\eta_+|^2)}+\frac{\lambda_5}{(\lambda_3+\lambda_5)(1+|\eta_-|^2)}\right)\Bigg] \tag{48}$$

and

$$P_{33} = 4\left[\frac{\lambda_2\lambda_3}{(\lambda_2+\lambda_3)}\frac{|\upsilon_+^*\upsilon_- - 1|^2}{(1+|\upsilon_+|^2)(1+|\upsilon_-|^2)}+\frac{\lambda_4\lambda_5}{(\lambda_4+\lambda_5)}\frac{|\eta_+^*\eta_- - 1|^2}{(1+|\eta_+|^2)(1+|\eta_-|^2)}\right], \tag{49}$$

where $\upsilon_\pm$ and $\eta_\pm$ are given in Eqs. (32) and (33), respectively. Also, we have $P_{12} = P_{21} = P_{23} = P_{32} = P_{13} = P_{31} = 0$.

IV. ANALYSIS OF QUANTUM CORRELATION DYNAMICS

In this section, we begin by studying the dynamics of quantum correlations characterized by negativity (24), UIN (38), and LQFI (47) for our qubit-qutrit mixed spin chain model under the local dephasing channels exhibiting Markovianity and non-Markovianity.

In Fig. 1, we show the temporal evolution of the negativity for several values of τ and different fixed values of the temperature $k_B T$ in the absence of the inhomogeneous magnetic field ($b/J = 0$). Note that we have set parameter $a = 1$ which acts as a system-environment coupling constant. So, the parameter $\tau > 2$ denotes the non-Markovian regime, whereas $\tau < 2$ corresponds to the Markovian regime. It can be seen that at a low-temperature regime ($k_B T = 0.01$), quantum entanglement estimated by the negativity is maximal [$\mathcal{N}(\rho(t, T)) = 1$] at $t = 0$ [see Fig. 1(a)], which means that the qubit-qutrit state is maximally entangled at the initial moment of interaction. Moreover, the entanglement decreases during the decoherence process until it reaches a steady-state value, which implies that the entanglement is frozen after a specific interval of time. For a smaller value of τ ($\tau = 0.5$ here), the negativity decreases asymptotically with tiny oscillations at a range of time. It is interesting to know that in the Markovian regime $\tau < 2$, we observe tiny revivals in entanglement evolution. As mentioned earlier, the parameter τ regulates the amount of information exchange between the system and the environment. Hence, the oscillations in the dynamical behavior of negativity are mostly controlled by τ. However, the Markovian regime accelerates the stabilization of the negativity. The decrement of the parameter τ causes the negativity to decay faster. With an increase in the temperature ($k_B T = 2$) [see Fig. 1(b)], the phenomena of ESD and ESB appear in the behavior of the negativity with a particular lower damped amplitude and reach a steady state, demonstrating the entanglement freezing phenomenon. Figure 1(c) shows that the dynamics of negativity do not exhibit rebirth for $\tau < 2$ when the temperature $k_B T = 3.5$ is assumed, showing that the system is in the Markovian regime. In this situation,

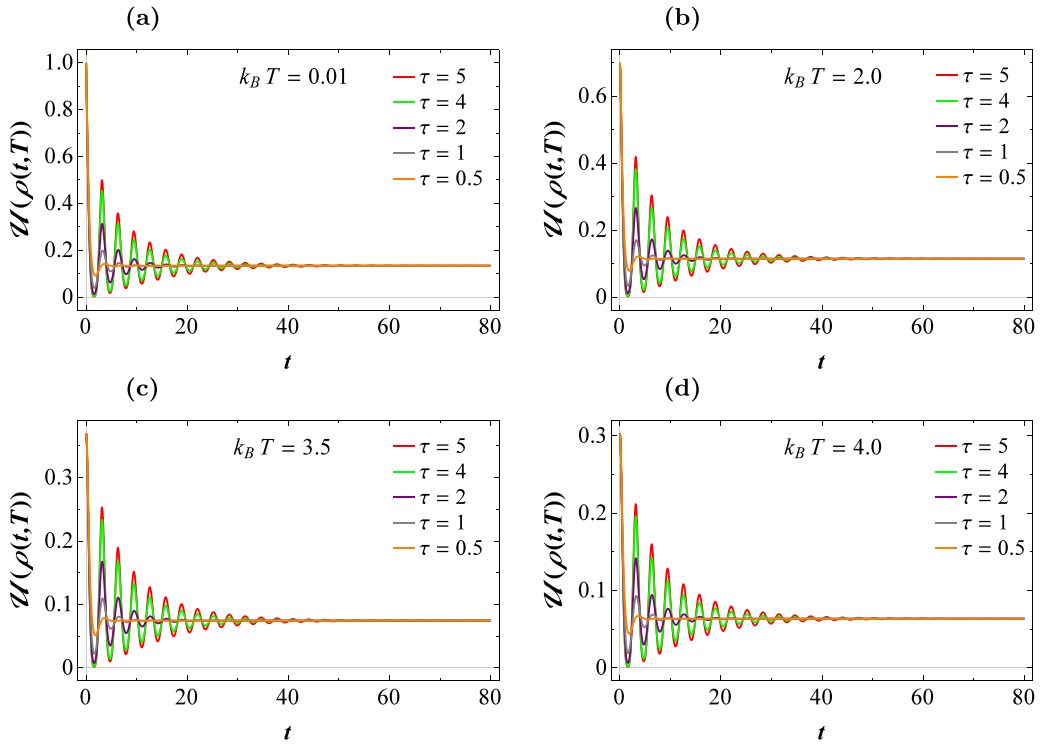

FIG. 2. Dynamics of the UIN versus t by considering a few different values of parameter τ at different values of the temperature k_BT/J, assuming fixed $\mu_B B/J = 0.5$, $D_z/J = 6$, $\Delta/J = 0.5$ when $b/J = 0$.

the entanglement between the qubit and qutrit becomes zero after a while, known as the ESD. For $\tau > 2$, the existence of ESD and ESB in the dynamical map of negativity indicates that the qubit-qutrit system and environment exchange information. In addition, such entanglement revivals indicate the usefulness of the parameter τ to convert free states or less entangled states to a more resourceful state (with a high degree of entanglement). In Fig. 1(d), we see that at a higher temperature $k_BT = 4$, for all considered values of τ, the ESD phenomenon appears. It must be noticed that as temperature increases, the entanglement saturates at lower values; specifically when $k_BT > 2$, the state becomes completely separable for the increasing interaction time. Further, we have shown that the lowest temperature values have a significant impact on the maximization of quantum entanglement. The temperature influences not only the initial entanglement of the system but also the non-Markovianity behavior. Lower values of the temperature allow the system to show non-Markovian effects and the entanglement decays with revival character. The presence of ESD and ESB in the current dynamical map of the entanglement estimator reveals that the system and the environment are highly interacting, exhibiting information exchange between them. In addition, practical transmitting channels can be fully fledged by exploiting the parameter τ to design longer entanglement preservation. As can be seen that when τ gets higher, the state's entanglement final saturation levels take time to diminish, hence preventing the state from the separability, in particular, for higher values of k_BT. It is noticeable that the magnetic field imposed on the dynamics of quantum systems without environmental noise is not equivalent to the current case with dephasing RT noise [58]. For example, it is intriguing to find that the total time of entanglement negativity becomes extended when injecting the RT noise. As seen in Ref. [58] without RT noise, the entanglement decays in a very short time as compared to that observed under the influence of RT noise. Besides, we observed the monotonic decay in the mentioned paper whereas, in the current case, the entanglement suffers repeated revivals due to the RT environmental dephasing effects, therefore completely contradicting the previous study of the similar system. Physically, this means that the current configuration is best suited for avoiding complete entanglement freezing by the conversion of free states to entangled resource states. However, the dynamics of the thermal entangled state in a qutrit-qubit mixed spin *XXZ* model when coupled to an external magnetic field have been in good agreement with current results by showing longer entanglement preservation along with oscillatory behavior [81].

Figure 2 depicts the dynamics of the mixed qubit-qutrit state using the UIN measure under the presence of an external magnetic field influenced by the RT noise. In the current case, we repeat the parameter values given in Fig. 1. In comparison, the dynamical behavior of UIN seems completely different from the negativity given in Fig. 1, specifically for higher values of the temperature k_BT. However, for a higher temperature regime, the UIN shows a set of damping oscillations with a series of revival and collapse phenomena over time with an asymptotic limit. Under the decoherence effects, the UIN decreases gradually to stabilize for a specific interval of time which means that the UIN becomes frozen. On the other hand, it is clear that even under the presence of the decoherence phenomenon, the monotonic decay does not occur in the behavior of UIN even in a high-temperature regime. This indicates the presence of nonlocality even in the absence of entanglement between the qubit and qutrit.

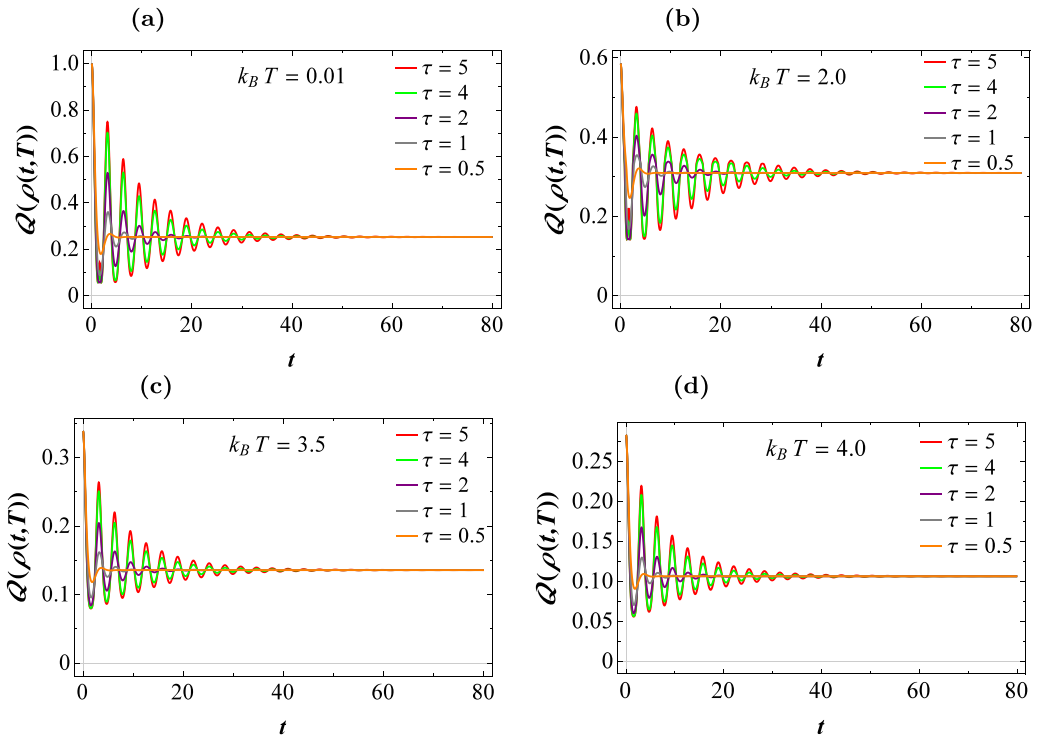

FIG. 3. Dynamics of the LQFI versus t by considering a few different values of parameter τ at different values of the temperature $k_B T/J$, assuming fixed $\mu_B B/J = 0.5$, $D_z/J = 6$, $\Delta/J = 0.5$ when $b/J = 0$.

This also implies that the ESD does not necessarily mean the loss of all quantum correlations. However, the fact remains the same and agrees with Fig. 1(a) that for low-temperature values $k_B T = 0.01$, the state becomes maximally correlated at $t = 0$ [see Fig. 2(a)]. Besides, the nonlocality measured via UIN shows strong resistance to any changes with temperature and nearly remains the same for all temperatures, except in the initial moments of interaction. The revival phenomenon is regulated by the parameter τ and not by any other parameter of the magnetic field in the current setup of parameters. However, slight revivals in the Markovian regime still exist due to the parameter τ which forces the environment to return the information to the system, making some revivals in the dynamical map of UIN. Furthermore, the revival character in the non-Markovian regime ensures the successful exchange of the attributes between the hybrid qubit-qutrit system and environment, which remains the reason to recover the nonlocality after the corresponding loss. The final saturation levels of the UIN measure completely depend upon the relevant temperature, and as temperature increases, the UIN tends to achieve the least values of the saturation levels, suggesting greater loss and vice versa. This is because temperature causes the state to be mixed and increases the entropy of the state, which finally results in greater nonlocality loss. Note that the dynamical maps of quantum correlations investigated under dephasing environments in Refs. [82,83] do not match with our results obtained by UIN, strong evidence of revivals and longer retention of quantum correlations. Besides, the final density matrices of the qubit-qutrit systems obtained in Refs. [82,83] have different structures as compared to that given in Eq. (16), indicating that the comparative configurations have a different amount of quantum correlations.

In Fig. 3, we address the dynamics of quantum correlation in terms of LQFI for a system of qubit-qutrit mixed spin chain coupled with an external magnetic field and superimposed by RT noise. For the current dynamical setup, we repeat the setting of the parameters used to obtain Fig. 1, but for LQFI. The qualitative dynamical outlook of the LQFI measure seems similar to that of the UIN criterion, however, with few slight changes. Namely, the maximum amount of quantum correlation captured by UIN for $t = 0$ is larger than that captured by LQFI. Not only the initial values of the quantum correlations, but the final saturation levels of the LQFI and UIN also do not match. Hence, this ensures that the nonlocality in terms of UIN differs from the quantum correlations quantified by LQFI. In comparison, the UIN and LQFI remain unfrozen and partially lost, which means that these two quantifiers go beyond quantum entanglement captured by negativity. In agreement with UIN, the related revival rate of LQFI increases for the increasing values of τ. Interestingly, the nonmonotonic decay of the LQFI occurs at the least values of τ; for instance, see the orange curves for $\tau = 0.5$. We notice a small revival of quantum correlation, which denotes the presence of feedback phenomenon in the environment causing a fraction of the lost information to flow back to the system at $\tau = 0.5$. Thus, as mentioned before, the low value of τ can also contribute to the behavioral dynamical maps of quantum correlations. The resultant decay in the current case resembles that obtained in the qubit-qutrit system when coupled to the magnetic field in Ref. [58] under the absence of environmental dephasing, where a shorter-lived and monotonic loss has been observed. However, we noticed that certain studies, such as Refs. [17,82,83], indicate that under the environmental dephasing, the decay observed is monotonic which again con-

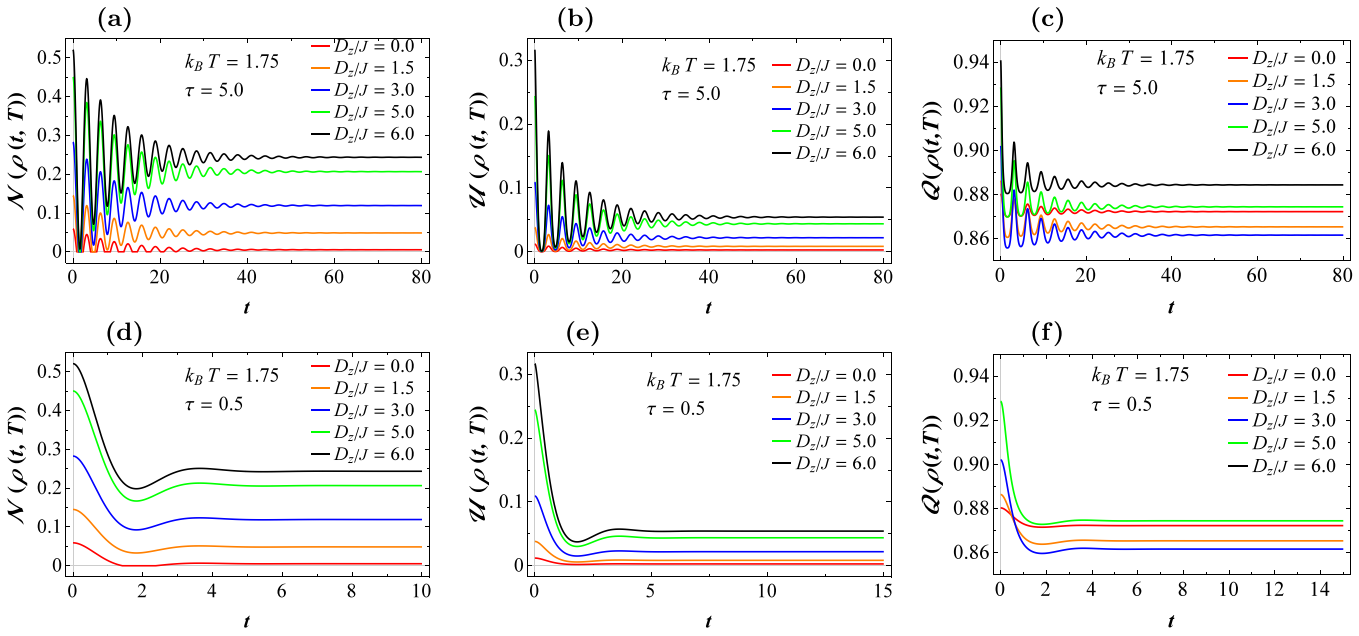

FIG. 4. Upper panels: The dynamics of quantum correlations versus t for several values of DM interaction at $\tau = 5$ when $\mu_B B/J = 0.5$, $k_B T/J = 1.75$, $\Delta/J = 0.5$, and $b/J = 0$. Lower panels: Same as upper panels but for $\tau = 0.5$.

trasts with the current results. Therefore, the longer quantum correlations and the presence of feedback phenomenon in the current system influenced by RT noise remained a more favorable resource for the quantum correlation transmission and preservation. Similarly, the study carried out in Ref. [81] resembles the current results where longer quantum correlation preservation in a qubit-qutrit system is modeled in two bosonic reservoirs regulated by temperature. For the increased efficiency of the quantum mechanical channels, one should increase τ, as it not only controls the revival's character but also regulates the preservation capacity of the system. As seen for higher values of τ, LQFI seems longer preserved. Note that the temperature variations strongly cause the initial quantum correlations to regulate and the two have been witnessed with an inverse relation. Furthermore, for each fixed value of temperature, the saturation level occurs at the same point even for different values of τ.

Figure 4 analyzes the dynamics of quantum correlations using negativity, UIN, and LQFI given in Eqs. (24), (38), and (47) in a mixed hybrid qubit-qutrit state exposed to an external magnetic field with reinforced RT noise. The external magnetic field here is described for different fixed values of DM interaction D_z when $k_B T = 1.75$, non-Markovian regime ($\tau = 5$) upper panel, Markovian regime ($\tau = 0.5$) lower panel, along with the absence of the inhomogeneity ($b = 0$). Because of the interplay of the DM interaction strength, the whole outlook of the comparative dynamics of negativity, UIN, and LQFI became changed. However, the impacts of the non-Markovianity and Markovianity as well as the temperature agree with Figs. 1–3. We observed that in the non-Markovian regime, the coupled fields allowed the quantum correlation quantifiers to decay in an oscillatory manner. Besides, the curves for high τ values took a longer time to saturate than for low values of the same parameter. In the Markovian regime, there occurs a single minimum of negativity, UIN, and LQFI for each parameter setting which then achieves its final saturation level. Also, because of no revivals of quantum phenomena, the loss of information and other attributes of the states will be assumed permanent, as no backflow of information occurs from the environment toward the system. For minimum temperature values, let $k_B T = 0.01$, we witness the state to be maximally correlated and vice versa, as seen in Figs. 1–3. In close connection with previous results, for the high value of temperature $k_B T = 1.75$, we detected the state to be partially entangled. We find the role of DM interaction strength opposite to that of the temperature, where the first one regulates the final saturation levels and the latter one, the initially encoded nonclassical correlations in the qubit-qutrit state. As seen for high values of D_z, the negativity and UIN remains highly preserved; however, for the least values, the forenamed quantities saturate at low values. Note that for $D_z/J = 0.0$, the state becomes completely classical and disentangled at the final interaction times. In contrast, with the LQFI, in the range $0 < D_z/J < 3.0$, we witness a contradicting behavior, where quantum correlations by means of LQFI show lesser loss at low values of D_z as compared to when $D_z/J = 3.0$. Note that for each value of D_z interaction strength, the LQFI initially as well as at final notes remains highly preserved and is not completely lost. This means that the LQFI is more resourceful to resist the dephasing effects of the RT noise and external magnetic field than entanglement and nonlocality, which were easily lost. Indeed, the DM interaction significantly enhances the amount of quantum correlations in the systems. This confirms the results reported in Ref. [62], in which the state become separable at lower values of the temperature in contrast to when the DM interaction is included in the system. Notably, the lower temperature and higher DM interaction strength also contributed to a single

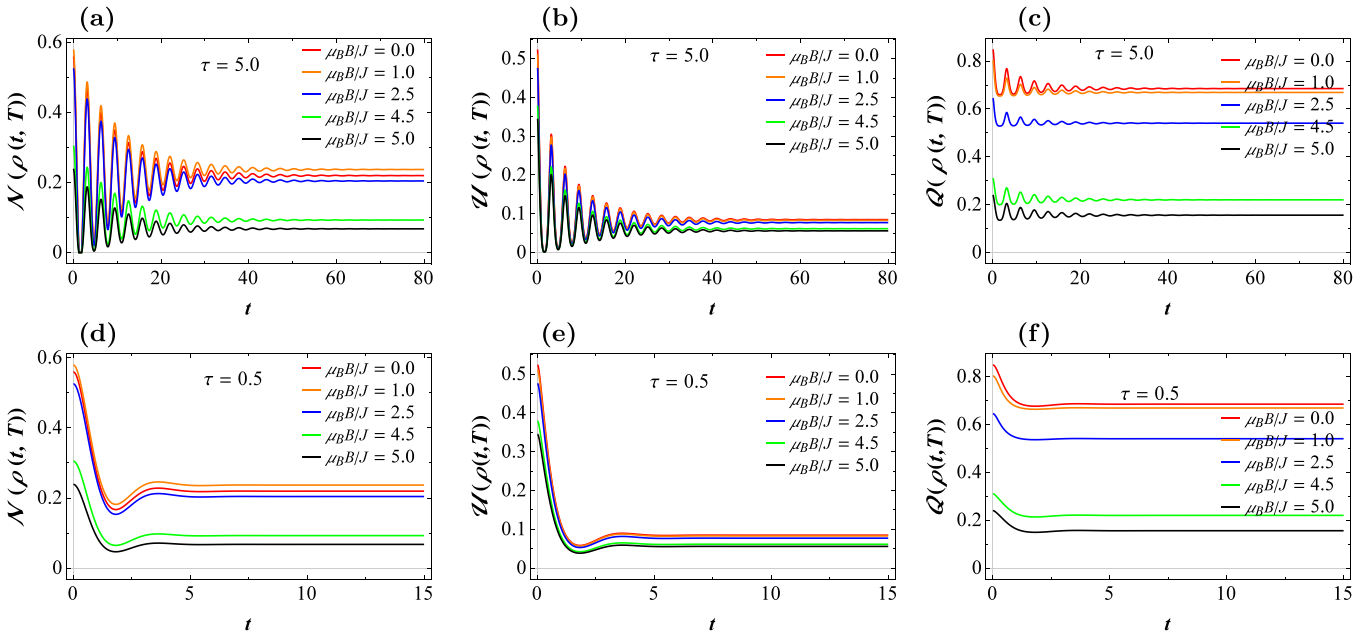

FIG. 5. Upper panels: The dynamics of quantum correlations versus t for several values of the external magnetic field at $\tau = 5$ when $D_z/J = 6$, $k_BT/J = 1.75$, $\Delta/J = 0.5$, and $b/J = 0$. Lower panels: Same as upper panels but for $\tau = 0.5$.

ESB, nonlocality, and LQFI even in the Markovian regime. We see that the negativity and UIN show a single revival after the first death.

Figure 5 illustrates the dynamics of negativity, UIN, and LQFI in a qubit-qutrit mixed entangled state when subjected to an external magnetic field and dephasing RT noise. We repeat the parameter settings shown in Fig. 4; however, we mainly focus on the effects of different fixed values of the magnetic field $\mu_B B/J$ on qubit-qutrit correlations retention in the state. The dynamical outlook of the negativity, UIN, and LQFI against increasing values of B seems opposed to that encountered against increasing D_z and τ values. For low values of $\mu_B B/J$, all quantifiers seemed better preserved. However, as the magnetic field strength increases, the correlations between the qubit-qutrit state become more suppressed. For instance, see the shifting of the red-lined curves to black end for increasing $\mu_B B/J$ values. Not only this, but the related revival rate of the correlation functions is also slightly decreased for the increasing values of B. Moreover, the maximums of the correlation functions against low values of $\mu_B B/J$ remain higher comparatively. We noticed a stronger revival rate in the dynamics of negativity, UIN, and LQFI for the higher values of τ in the non-Markovian regime. A faster decline of the quantum correlations has been witnessed in the Markovian regimes with a single minimum, as one can see that the negativity, UIN, and LQFI achieve the final saturation values quicker compared to that in the non-Markovian regime. Because of the revival phenomenon, the correlations in the system remain preserved for longer intervals in the non-Markovian regime. As compared to the negativity and UIN measures, the LQFI has been found highly impacted by the external magnetic field. The statement is followed by the fact that the revival character of the LQFI vanishes faster compared to that observed for negativity and UIN. Notably, in the Markovian regime, the LQFI fully exhibits an exponential decay before saturating at a constant value, which is comparable to the results of the negativity and UIN. However, it is still noticeable that the LQFI estimator encounters quantum correlations with larger initial values, which are followed by negativity and then UIN. Thus, one can conclude that the current hybrid state has greater initially encoded LQFI than entanglement and nonlocality. Remarkably, in the Markovian regime, a smaller revival character of the entanglement, nonlocality, and LQFI is observed. This is due to the fact that the parameter τ supports a single exchange of information between the system and the environment.

Figure 6 explores the dynamics of nonclassical correlations in a qubit-qutrit hybrid mixed thermal entangled state when an inhomogeneous magnetic field is applied along with RT noise either with Markovian or non-Markovian character. We primarily focus on the impact prevailed by the degree of inhomogeneity on preservation and behavioral dynamics of negativity, UIN, and LQFI. The overall dynamical map of the negativity and LQFI seems opposite in the current case as compared to that observed against B except for UIN. The fact that the increase in homogeneity increases the decay followed the statement. However, the inhomogeneity helps to avoid greater losses and the decay levels become lesser as the related parameter b is increased. In addition, we noticed that the inhomogeneity causes no changes to the revival character of the qubit-qutrit correlations and remained ineffective. The revival character depends upon the parameter τ and the related temperature of the reservoir and agrees with Figs. 1–5. The final decay levels for each inhomogeneous magnetic field strength parameter b are varied and as it increases, the decay levels indicate lesser degradation of the current qubit-qutrit correlations. Nevertheless, UIN remains susceptible to the strength of parameter b and as it grows, the related decay also increases, demonstrating the contradicting behavior to negativity and LQFI. Therefore, we conclude that not all the qubit-qutrit

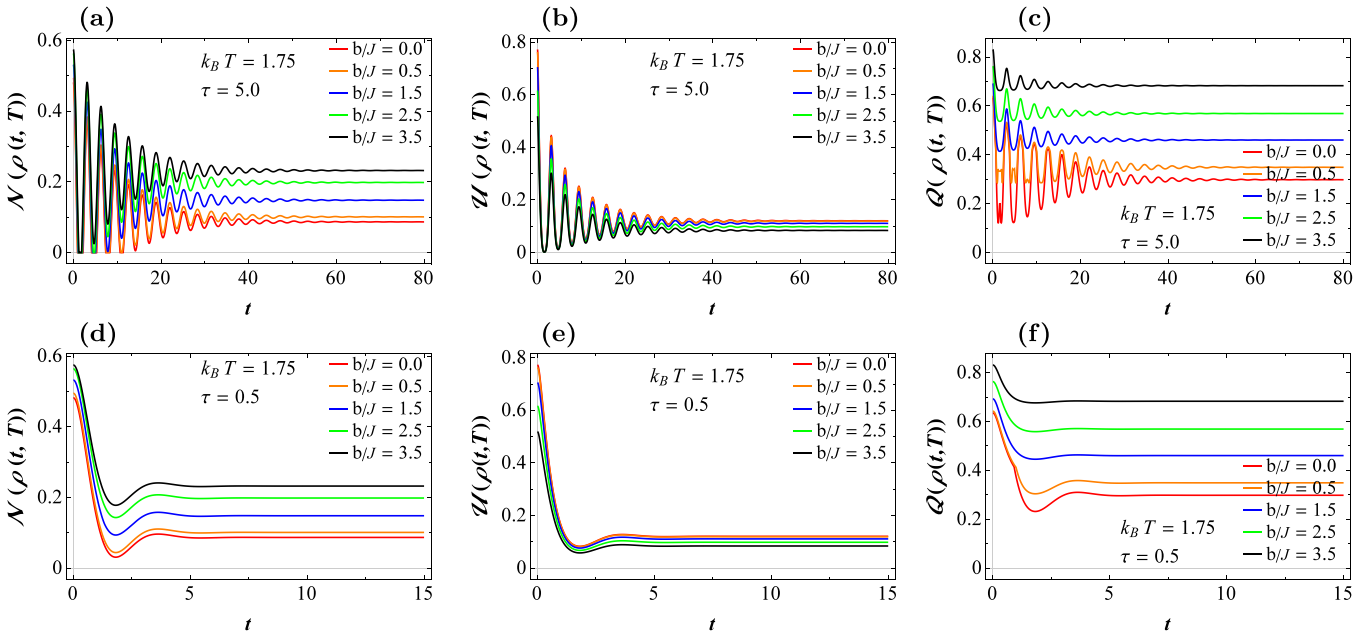

FIG. 6. Upper panels: The dynamics of quantum correlations versus t for several values of an inhomogeneous magnetic field at $\tau = 5$ when $D_z/J = 6$, $k_BT/J = 1.75$, $\Delta/J = 0.5$, and $\mu_B B/J = 0.5$. Lower panels: Same as upper panels but for $\tau = 0.5$.

correlations are equivalent, ensuring their different nature and that similar features of the magnetic field can differently affect them. In the Markovian regime, we notice that for the increasing values of b, the amplitude of the single observed minima increases for the case of negativity and LQFI; however, the opposite occurs in the case of UIN. Note that the mixed entangled state does not become fully separable and attains a final saturation level. The only reason behind this is setting the DM interaction and exchange parameter J to high values which avoid the full separability of the state. The existence of the revival character in the non-Markovian regime indicates the exchange of attributes between the hybrid-spin system and the environment, resulting in temporary information decay for a definite interval. Nonetheless, in the Markovian regime, we witness no revivals which will cause permanent information decay. However, the existence of slight revivals in the Markovian regime is due to the parameter τ, as the width of the Markovian regime is defined by the dimensionless product $a\tau$ (with $a = 1$). Therefore, there are still signs of the revivals in the regime where $\tau < 2$, causing the backflow of information from the environment to the system.

In Fig. 7, we address the time evolution of negativity, UIN, and LQFI for a system of hybrid-spin structure including a qubit-qutrit mixed entangled thermal state coupled with an external magnetic field. In the current case, we mainly focus on the temperature influence on the qubit-qutrit system dynamics. Temperature greatly influenced the initial negativity, UNI, and LQFI values and for the increasing values of T, the initially encoded correlations in the state become suppressed. This means that the rise in temperature makes the system more and more mixed rather than entangled. It is important to note that the initial negativity, UIN, and LQFI varies in magnitudes. In comparison, the initial qubit-qutrit correlations remain more resistant to the temperature effects. More explicitly, the higher values of temperature have negatively influenced the entanglement and it becomes easily lost at high-temperature values. On the other hand, the nonlocality is not completely lost even for the higher values of the temperature. In the case of LQFI, the related final saturation levels show comparatively the least decay because of the higher as well as the lower values of temperature. The results for non-Markovian and Markovian regimes remain in agreement with those defined in Figs. 4–6 and suggest strong revivals in the former and monotonic pattern decay in the latter. In light of the above results, we conclude that characterizing the Hamiltonian parameters by different features can be usefully utilized for practical quantum information processing. In addition, we find the least temperature values more resourceful to induce maximum qubit-qutrit correlations initially. Not only this, but the low-temperature values also contribute to longer quantum correlations preservation in the system. It can be seen that at low temperatures, the non-Markovian behavior is more obvious as compared to that at higher values. Therefore, besides parameter τ, the temperature also severally affects the non-Markovian dynamical maps of quantum correlations. However, some revivals exist in the Markovian regime, due to the system-environment coupling. This causes the information to exchange between the qubit-qutrit system and the environment even in the Markovian regime, implying the non-monotonic oscillatory behavior in negativity, nonlocality, and quantum Fisher information.

V. FINAL REMARKS

Now we consider comparing the current dynamical maps of quantum correlations to that observed for different quantum systems studied previously. In Ref. [84], the dynamics of entanglement and coherence for a system of three qubits, when coupled to external local fields, have been shown under the power-law and RT noises with a higher non-Markovian

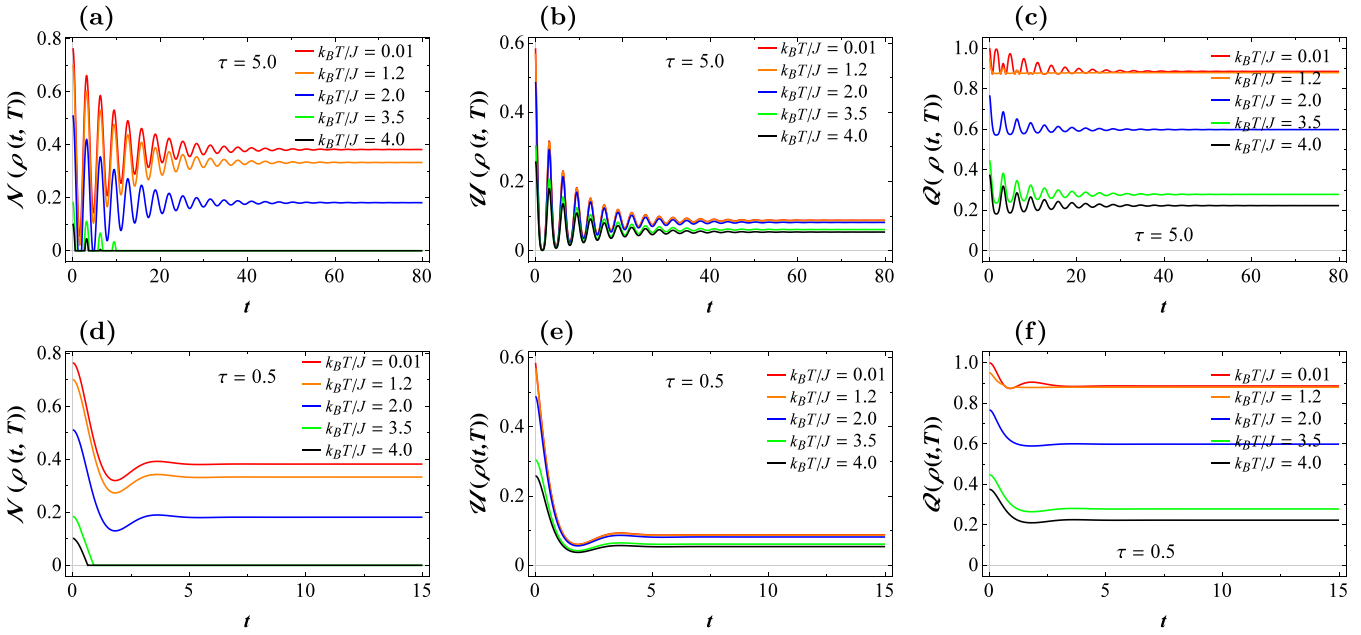

FIG. 7. Upper panels: The dynamics of quantum correlations versus t for several values of the temperature at $\tau = 5$ when $\mu_B B/J = 0.5$, $D_z/J = 6$, $b/J = 3.5$, and $\Delta/J = 0.5$. Lower panels: Same as upper panels but for $\tau = 0.5$.

behavior and preservation capacity as compared to that observed in the current case. Also, in the case of tripartite maximally entangled state when exposed to the classical field and mixed RT and static noise, the resultant exchange capacity and preservation intervals witnessed were comparatively reduced [85]. In the current case, we encountered a smaller exchange of information in the Markovian regime, which was completely absent for different quantum systems under the influence of RT noise in Refs. [38,84,85]. The Markovian and non-Markovian characteristics in the current case were exploited by the different aspects of the magnetic field and the resultant effects were completely changed. For example, in the non-Markovian regime, when the temperature is raised, the oscillatory behavior vanishes, whereas, when the Markovian regime is employed with low temperature, we observed some revivals in quantum correlations. This means that the Markovian and non-Markovian properties can be exploited and can be traced back to the similar results obtained in Ref. [86] for a system of two qubits exposed to mixed dephasing noises. It is important to note that the current qubit-qutrit system performed better at showing greater preservation of quantum correlations as compared to the two-qubit, three-qubit, free, and bound two-qutrit systems studied in Refs. [38,85–88].

In addition, it is also important to note that the current results obtained for negativity, UIN, and LQFI are found matching with other quantum phenomena. For instance, in Ref. [89], the generation of entropic uncertainty is found inversely dependent upon the existence of quantum correlations between the subquantum systems of the neutrino-flavor state. We observed repeated revivals of quantum correlations; therefore, in agreement with Ref. [89], there is a probability of generation of quantum memory in the current qubit-qutrit entangled state also. In Ref. [90], the authors proposed a trade-off scheme that revealed the complementarity relation between first-order coherence and intrinsic concurrence. Hence, providing a theoretical basis for reliable quantum information processing and preservation resources is valuable. Compared to the current case, there is a direct relation between entanglement, nonlocality, and LQFI. Accordingly, it is also a prospect of the current study to demonstrate the relations between first-order coherence and intrinsic concurrence in the qubit-qutrit systems. Furthermore, we find several other quantum criteria influencing each other directly or indirectly. These include the relation of coherence with entropic uncertainty, decoherence effects raised by the rising quantum memory generation values, and the influence of spin chains and related field parameters on the generation of quantum memory in quantum systems [91–93]. In light of these references, we find that the currently studied quantum correlations and related dynamical maps will strengthen bonds with the emerging values of quantum memory assisted entropic uncertainty and coherence [94,95]. Thereby, we believe that all of these studies are strong candidates for the future prospects of the current qubit-qutrit states and might yield interesting results.

VI. CONCLUSION

Quantum information processing and computing require longer preservation of the resources like entanglement, nonlocality, and other quantum correlations. This could be done by investigating different types of external transmitting mediums, related manipulation, and characterization of the parameters. In this study, we are motivated to investigate a thermal hybrid qubit-qutrit mixed entangled state coupled with an external magnetic field and dephasing RT noise. Using negativity, uncertainty-induced nonlocality, and local quantum Fisher information, we analyzed the dynamics and preservation of quantum correlations. With the optimal values of parameters, one can design longer preservation as well as the optimal

dynamical map of quantum correlations in a nonlocal setup. Therefore, we aim to provide optimal values of the related parameters to induce higher preservation of quantum correlations and optimal dynamical behavior.

Our findings show that when characterized by RT dephasing noise, the characteristic behavior of the external magnetic field towards the preservation and dynamics of the qubit-qutrit correlations changes. The characterization of the applied magnetic field by RT noise enables us to induce easy non-Markovian or Markovian dynamics, which seem completely different from conventional magnetic fields and related effects. Moreover, for certain parameters, for example, at high values of DM interaction strength, the non-Markovianity remained the only reason for the entanglement, nonlocality, and quantum correlation preservation in the state. However, this non-Markovianity is detected fragile to the temperature and is suppressed by the related action. Besides this, the temperature has been recorded to regulate the initial quantum correlations in the state and the two have been found in an indirect relation. In particular, characterizing the magnetic field by different parameters affects the qubit-qutrit correlations differently. For instance, the quantum correlations computed by local quantum Fisher information stand as the most effective one and showed the least decay when influenced by DM interaction, magnetic field strength, and temperature. The entanglement and nonlocality measured by negativity and uncertainty-induced nonlocality both remained weaker when exposed to the magnetic field, temperature, and even when DM interaction comes into interplay. According to our results, the optimal parameters which can boost the initial quantum correlations and can preserve them for longer are when the external magnetic field is characterized by the higher DM interaction and inhomogeneity strength at low temperatures. Finally, we found that the current transmitting and preservation channels, i.e., the magnetic field superimposed with RT noise, are vital resources for inducing larger quantum correlation preservation. Most importantly, the current coupled fields have many advantages, which can be used to produce the optimally required kind of dynamical maps of the quantum phenomena.

All data generated or analyzed during this study are included in this paper.

ACKNOWLEDGMENTS

F.B. has put forward the main idea for the model and method and performed the calculations and graphical tasks. A.U.R. and S.H. have contributed to interpreting the results and writing the manuscript. Thorough checking of the manuscript and confirming the conclusions were done by S.H. and A.U.R. The final draft of the manuscript was revised by S.H. and reviewed by all authors.

The authors declare no competing interests.

[1] K. Bu, A. Kumar, L. Zhang, and J. Wu, Cohering power of quantum operations, Phys. Lett. A **381**, 1670 (2017).

[2] K. C. Tan, H. Kwon, C. Y. Park, and H. Jeong, Unified view of quantum correlations and quantum coherence, Phys. Rev. A **94**, 022329 (2016).

[3] D. Beckman, D. Gottesman, M. A. Nielsen, and J. Preskill, Causal and localizable quantum operations, Phys. Rev. A **64**, 052309 (2001).

[4] A. Brodutch and K. Modi, Criteria for measures of quantum correlations, Quantum Inf. Comput. **12**, 721 (2012).

[5] U. Khalid, J. ur Rehman, and H. Shin, Measurement-based quantum correlations for quantum information processing, Sci. Rep. **10**, 2443 (2020).

[6] A. Bokulich and G. Jaeger, *Philosophy of Quantum Information and Entanglement* (Cambridge University Press, Cambridge, 2010).

[7] R. Ursin, F. Tiefenbacher, T. Schmitt-Manderbach, H. Weier, T. Scheidl, M. Lindenthal, and A. Zeilinger, Entanglement-based quantum communication over 144 km, Nat. Phys. **3**, 481 (2007).

[8] G. Arun and V. Mishra, A review on quantum computing and communication, in *2014 2nd International Conference on Emerging Technology Trends in Electronics, Communication and Networking* (IEEE, Surat, India, 2014).

[9] L. Gyongyosi and S. Imre, A survey on quantum computing technology, Comput. Sci. Rev. **31**, 51 (2019).

[10] C. H. Bennett, G. Brassard, C. Crépeau, R. Jozsa, A. Peres, and W. K. Wootters, Teleporting an Unknown Quantum State via Dual Classical and Einstein-Podolsky-Rosen Channels, Phys. Rev. Lett. **70**, 1895 (1993).

[11] H. Zhang, Z. Ji, H. Wang, and W. Wu, Survey on quantum information security, China Commun. **16**, 1 (2019).

[12] R. B. Jin, M. Takeoka, U. Takagi, R. Shimizu, and M. Sasaki, Highly efficient entanglement swapping and teleportation at telecom wavelength, Sci. Rep. **5**, 9333 (2015).

[13] Z. Ji, H. Zhang, and P. Fan, Two-party quantum private comparison protocol with maximally entangled seven-qubit state, Mod. Phys. Lett. A **34**, 1950229 (2019).

[14] Z. Ji, P. Fan, H. Zhang, and H. Wang, Greenberger-Horne-Zeilinger-based quantum private comparison protocol with bit-flipping, Phys. Scr. **96**, 015103 (2021).

[15] S. Bose, M. B. Plenio, and V. Vedral, Mixed state dense coding and its relation to entanglement measures, J. Mod. Opt. **47**, 291 (2000).

[16] A. A. Katanin, A. S. Belozerov, and V. I. Anisimov, Nonlocal correlations in the vicinity of the α-γ phase transition in iron within a DMFT plus spin-fermion model approach, Phys. Rev. B **94**, 161117(R) (2016).

[17] M. Jafarpour, F. K. Hasanvand, and D. Afshar, Dynamics of entanglement and measurement-induced disturbance for a hybrid qubit-qutrit system interacting with a spin-chain environment: A mean field approach, Commun. Theor. Phys. **67**, 27 (2017).

[18] K. K. Sharma and S. N. Pandey, Dynamics of entanglement in qubit-qutrit with x-component of DM interaction, Commun. Theor. Phys. **65**, 278 (2016).

[19] A. U. Rahman, M. Noman, M. Javed, M. X. Luo, and A. Ullah, Quantum correlations of tripartite entangled states under Gaussian noise, Quant. Info. Proc. **20**, 290 (2021).

[20] A. U. Rahman, M. Javed, A. Ullah, and Z. Ji, Probing tripartite entanglement and coherence dynamics in pure and mixed

independent classical environments, Quantum Inf. Process. **20**, 321 (2021).

[21] A. U. Rahman, M. Noman, M. Javed, A. Ullah, and M. X. Luo, Effects of classical fluctuating environments on decoherence and bipartite quantum correlations dynamics, Laser Phys. **31**, 115202 (2021).

[22] A. T. Tsokeng, M. Tchoffo, and L. C. Fai, Dynamics of entanglement and quantum states transitions in spin-qutrit systems under classical dephasing and the relevance of the initial state, J. Phys. Commun. **2**, 035031 (2018).

[23] S. Haddadi, A brief note on the Scott measure as a multipartite entanglement criterion, Laser Phys. Lett. **17**, 075201 (2020).

[24] B. M. Li, M. L. Hu, and H. Fan, Nonlocal advantage of quantum coherence and entanglement of two spins under intrinsic decoherence, Chin. Phys. B **30**, 070307 (2021).

[25] F. Benabdallah, A. Slaoui, and M. Daoud, Quantum discord based on linear entropy and thermal negativity of qutrit-qubit mixed spin chain under the influence of external magnetic field, Quantum Inf. Process. **19**, 252 (2020).

[26] P. J. Van Koningsbruggen, O. Kahn, K. Nakatani, Y. Pei, J. P. Renard, M. Drillon, and P. Legoll, Magnetism of A-Cu^{II} bimetallic chain compounds (A = Fe, Co, Ni): One- and three-dimensional behaviors, Inorg. Chem. **29**, 3325 (1990).

[27] T. Boness, S. Bose, and T. S. Monteiro, Entanglement and Dynamics of Spin Chains in Periodically Pulsed Magnetic Fields: Accelerator Modes, Phys. Rev. Lett. **96**, 187201 (2006).

[28] A. Redwan, A. H. Abdel-Aty, and N. Zidan, Dynamics of classical and quantum information on spin-chains with multiple interactions, Inf. Sci. Lett. **7**, 1 (2018).

[29] M. L. Hu, Y. Y. Gao, and H. Fan, Steered quantum coherence as a signature of quantum phase transitions in spin chains, Phys. Rev. A **101**, 032305 (2020).

[30] S. Haseli, S. Haddadi, and M. R. Pourkarimi, Entropic uncertainty lower bound for a two-qubit system coupled to a spin chain with Dzyaloshinskii-Moriya interaction, Opt. Quantum Electron. **52**, 465 (2020).

[31] S. Haddadi and A. Akhound, Thermal entanglement properties in two qubits one-axis spin squeezing model with an external magnetic field, Int. J. Theor. Phys. **58**, 399 (2019).

[32] D. Wang, F. Ming, A. J. Huang, W. Y. Sun, and L. Ye, Entropic uncertainty for spin-1/2XXX chains in the presence of inhomogeneous magnetic fields and its steering via weak measurement reversals, Laser Phys. Lett. **14**, 095204 (2017).

[33] M. J. Uren, D. J. Day, and M. Kirton, $1/f$ and random telegraph noise in silicon metal-oxide-semiconductor field-effect transistors, Appl. Phys. Lett. **47**, 1195 (1985).

[34] A. U. Rahman, M. Noman, M. Javed, and A. Ullah, Dynamics of bipartite quantum correlations and coherence in classical environments described by pure and mixed Gaussian noises, Eur. Phys. J. Plus **136**, 846 (2021).

[35] S. Daniotti, C. Benedetti, and M. G. Paris, Qubit systems subject to unbalanced random telegraph noise: Quantum correlations, non-Markovianity and teleportation, Eur. Phys. J. D **72**, 208 (2018).

[36] E. Paladino, Y. M. Galperin, G. Falci, and B. L. Altshuler, $1/f$ noise: Implications for solid-state quantum information, Rev. Mod. Phys. **86**, 361 (2014).

[37] X. Cai, Quantum dephasing induced by non-Markovian random telegraph noise, Sci. Rep. **10**, 88 (2020).

[38] A. T. Tsokeng, M. Tchoffo, and L. C. Fai, Quantum correlations and decoherence dynamics for a qutrit-qutrit system under random telegraph noise, Quantum Inf. Process. **16**, 191 (2017).

[39] T. Aoki, Y. Nishikawa, and M. Kuwata-Gonokami, Room-temperature random telegraph noise in luminescence from macroscopic InGaN clusters, Appl. Phys. Lett. **78**, 1065 (2001).

[40] G. Burkard, Non-Markovian qubit dynamics in the presence of $1/f$ noise, Phys. Rev. B **79**, 125317 (2009).

[41] F. Liu and K. L. Wang, Correlated random telegraph signal and low-frequency noise in carbon nanotube transistors, Nano Lett. **8**, 147 (2008).

[42] S. Cialdi, C. Benedetti, D. Tamascelli, S. Olivares, M. G. Paris, and B. Vacchini, Experimental investigation of the effect of classical noise on quantum non-Markovian dynamics, Phys. Rev. A **100**, 052104 (2019).

[43] M. Lewenstein, B. Kraus, J. I. Cirac, and P. Horodecki, Optimization of entanglement witnesses, Phys. Rev. A **62**, 052310 (2000).

[44] W. K. Wootters, Entanglement of formation and concurrence, Quantum Inf. Comput. **1**, 27 (2001).

[45] S. Luo, Quantum discord for two-qubit systems, Phys. Rev. A **77**, 042303 (2008).

[46] S. Haddadi and M. Bohloul, A brief overview of bipartite and multipartite entanglement measures, Int. J. Theor. Phys. **57**, 3912 (2018).

[47] M. L. Hu, X. Hu, J. Wang, Y. Peng, Y. R. Zhang, and H. Fan, Quantum coherence and geometric quantum discord, Phys. Rep. **762–764**, 1 (2018).

[48] D. Girolami, T. Tufarelli, and G. Adesso, Characterizing Nonclassical Correlations via Local Quantum Uncertainty, Phys. Rev. Lett. **110**, 240402 (2013).

[49] S. Kim, L. Li, A. Kumar, and J. Wu, Characterizing nonclassical correlations via local quantum Fisher information, Phys. Rev. A **97**, 032326 (2018).

[50] R. L. Xiao, X. Xiao, and W. J. Zhong, Dynamics of measurement-induced non-locality and geometric discord with initial system–environment correlations, Chin. Phys. B **22**, 080306 (2013).

[51] P. Calabrese, J. Cardy, and E. Tonni, Entanglement Negativity in Quantum Field Theory, Phys. Rev. Lett. **109**, 130502 (2012).

[52] A. B. A. Mohamed and E. M. Khalil, Atomic non-locality dynamics of two moving atoms in a hybrid nonlinear system: Concurrence, uncertainty-induced non-locality and Bell inequality, Opt. Quantum Electron. **53**, 612 (2021).

[53] M. Hagiwara, Y. Narumi, K. Minami, K. Tatani, and K. Kindo, Magnetization process of the $S = 1/2$ and 1 ferrimagnetic chain and dimer, J. Phys. Soc. Jpn. **68**, 2214 (1999).

[54] H. Čenčariková and J. Strečka, Unconventional strengthening of the bipartite entanglement of a mixed spin-(1/2, 1) Heisenberg dimer achieved through Zeeman splitting, Phys. Rev. B **102**, 184419 (2020).

[55] R. Demkowicz-Dobrzański, W. Górecki, and M. Guţă, Multi-parameter estimation beyond quantum Fisher information, J. Phys. A: Math. Theor. **53**, 363001 (2020).

[56] Y. Du, L. Jing, H. Fang, H. Chen, Y. Cai, R. Wang, and Z. Ji, Exploring the impact of random telegraph noise-induced accuracy loss on resistive RAM-based deep neural network, IEEE Trans. Electron Devices **67**, 3335 (2020).

[57] H. T. Lu, Y. J. Wang, S. Qin, and T. Xiang, Zigzag spin chains with antiferromagnetic-ferromagnetic interactions:

Transfer-matrix renormalization group study, Phys. Rev. B **74**, 134425 (2006).
[58] S. Xu, X. K. Song, and L. Ye, Measurement-induced disturbance and negativity in mixed-spin *XXZ* model, Quantum Inf. Process. **13**, 1013 (2014).
[59] S. Daffer, K. Wodkiewicz, J. D. Cresser, and J. K. Mclver, Depolarizing channel as a completely positive map with memory, Phys. Rev. A **70**, 010304(R) (2004).
[60] J. P. G. Pinto, G. Karpat, and F. F. Fanchini, Sudden change of quantum discord for a system of two qubits, Phys. Rev. A **88**, 034304 (2013).
[61] M. Ali, Dynamics of genuine multipartite entanglement under local non-Markovian dephasing, Phys. Lett. A **378**, 2048 (2014).
[62] F. Benabdallah, H. Arian Zad, M. Daoud, and N. Ananikian, Dynamics of quantum correlations in a qubit-qutrit spin system under random telegraph noise, Phys. Scr. **96**, 125116 (2021).
[63] Ł. Cywiński, R. M. Lutchyn, C. P. Nave, and S. D. Sarma, How to enhance dephasing time in superconducting qubits, Phys. Rev. B **77**, 174509 (2008).
[64] M. A. Nielson and I. L. Chuang, *Quantum Computation and Quantum Information* (Cambridge University Press, Cambridge, 2000).
[65] F. Benabdallah and M. Daoud, Dynamics of quantum discord based on linear entropy and negativity of qutrit-qubit system under classical dephasing environments, Eur. Phys. J. D **75**, 3 (2021).
[66] H. P. Breuer and F. Petruccione, *The Theory of Open Quantum Systems* (Oxford University Press, Oxford, 2002).
[67] G. Vidal and R. F. Werner, Computable measure of entanglement, Phys. Rev. A **65**, 032314 (2002).
[68] A. Peres, Separability Criterion for Density Matrices, Phys. Rev. Lett. **77**, 1413 (1996).
[69] M. Horodecki, P. Horodecki, and R. Horodecki, Separability of mixed states: Necessary and sufficient conditions, Phys. Lett. A **223**, 1 (1996).
[70] E. P. Wigner and M. M. Yanase, Information contents of distributions, Proc. Natl. Acad. Sci. USA **49**, 910 (1963).
[71] S. X. Wu, J. Zhang, C. S. Yu, and H. S. Song, Uncertainty-induced quantum nonlocality, Phys. Lett. A **378**, 344 (2014).
[72] Y. Khedif, S. Haddadi, M. R. Pourkarimi, and M. Daoud, Thermal correlations and entropic uncertainty in a two-spin system under DM and KSEA interactions, Mod. Phys. Lett. A **36**, 2150209 (2021).
[73] M. Ali, Local quantum uncertainty for multipartite quantum systems, Eur. Phys. J. D **74**, 186 (2020).
[74] A. Fujiwara and H. Nagaoka, Quantum Fisher metric and estimation for pure state models, Phys. Lett. A **201**, 119 (1995).
[75] M. G. A. Paris, Quantum estimation for quantum technology, Int. J. Quantum Inf. **07**, 125 (2009).
[76] S. L. Braunstein and C. M. Caves, Statistical Distance and the Geometry of Quantum States, Phys. Rev. Lett. **72**, 3439 (1994).
[77] D. Girolami, A. M. Souza, V. Giovannetti, T. Tufarelli, J. G. Filgueiras, R. S. Sarthour, D. O. Soares-Pinto, I. S. Oliveira, and G. Adesso, Quantum Discord Determines the Interferometric Power of Quantum States, Phys. Rev. Lett. **112**, 210401 (2014).
[78] H. S. Dhar, M. N. Bera, and G. Adesso, Characterizing non-Markovianity via quantum interferometric power, Phys. Rev. A **91**, 032115 (2015).
[79] S. Elghaayda, Z. Dahbi, and M. Mansour, Local quantum uncertainty and local quantum Fisher information in two-coupled double quantum dots, Opt. Quantum Electron. **54**, 419 (2022).
[80] F. Benabdallah, K. E. Anouz, and M. Daoud, Toward the relationship between local quantum Fisher information and local quantum uncertainty in the presence of intrinsic decoherence, Eur. Phys. J. Plus **137**, 548 (2022).
[81] L. Chen, X. Q. Shao, and S. Zhang, Measurement-induced disturbance and nonequilibrium thermal entanglement in a qutrit-qubit mixed spin *XXZ* model, Chin. Phys. B **20**, 100311 (2011).
[82] H. Yuan and L. F. Wei, Dynamics of measurement-induced disturbance for a qubit-qutrit system in noninertial frames, Commun. Theor. Phys. **59**, 17 (2013).
[83] A. Basit, H. Ali, F. Badshah, and G. Q. Ge, Enhancement of quantum correlations in qubit-qutrit systems under the non-Markovian environment, Commun. Theor. Phys. **68**, 29 (2017).
[84] A. U. Rahman, S. Haddadi, and M. R. Pourkarimi, Tripartite quantum correlations under power-law and random telegraph noises: Collective effects of Markovian and non-Markovian classical fields, Ann. Phys. (Berlin) **534**, 2100584 (2022).
[85] L. T. Kenfack, M. Tchoffo, G. C. Fouokeng, and L. C. Fai, Dynamics of tripartite quantum correlations in mixed classical environments: The joint effects of the random telegraph and static noises, Int. J. Quantum Inf. **15**, 1750038 (2017).
[86] M. Javed, S. Khan, and S. A. Ullah, The dynamics of quantum correlations in mixed classical environments, J. Russ. Laser Res. **37**, 562 (2016).
[87] A. T. Tsokeng, M. Tchoffo, and L. C. Fai, Free and bound entanglement dynamics in qutrit systems under Markov and non-Markov classical noise, Quantum Inf. Process. **17**, 190 (2018).
[88] S. Haddadi, M. R. Pourkarimi, and D. Wang, Tripartite entropic uncertainty in an open system under classical environmental noise, J. Opt. Soc. Am. B **38**, 2620 (2021).
[89] D. Wang, F. Ming, X. K. Song, L. Ye, and J. L. Chen, Entropic uncertainty relation in neutrino oscillations, Eur. Phys. J. C **80**, 800 (2020).
[90] F. Ming, D. Wang, L. J. Li, X. G. Fan, X. K. Song, L. Ye, and J. L. Chen, Tradeoff relations in quantum resource theory, Adv. Quantum Technol. **4**, 2100036 (2021).
[91] F. Ming, D. Wang, A. J. Huang, W. Y. Sun, and L. Ye, Decoherence effect on quantum-memory-assisted entropic uncertainty relations, Quantum Inf. Process. **17**, 9 (2018).
[92] Y. N. Guo, M. F. Fang, and K. Zeng, Entropic uncertainty relation in a two-qutrit system with external magnetic field and Dzyaloshinskii-Moriya interaction under intrinsic decoherence, Quantum Inf. Process. **17**, 187 (2018).
[93] A. B. A. Mohamed, A. N. Khedr, S. Haddadi, A. U. Rahman, M. Tammam, and M. R. Pourkarimi, Intrinsic decoherence effects on nonclassical correlations in a symmetric spin-orbit model, Results Phys. **39**, 105693 (2022).
[94] F. Ming, D. Wang, W. N. Shi, A. J. Huang, M. M. Du, W. Y. Sun, and L. Ye, Exploring uncertainty relation and its connection with coherence under the Heisenberg spin model with the Dzyaloshinskii-Moriya interaction, Quantum Inf. Process. **17**, 267 (2018).
[95] S. Haddadi, M. R. Pourkarimi, and S. Haseli, Relationship between quantum coherence and uncertainty bound in an arbitrary two-qubit X-state, Opt. Quantum Electron. **53**, 529 (2021).